Appl Phys B (2011) 103:907–916
DOI 10.1007/s00340-011-4487-2

Applied Physics B
Lasers and Optics

Distributed feedback dye laser holographically induced in improved organic–inorganic photocurable nanocomposites

O.V. Sakhno · J. Stumpe · T.N. Smirnova

Received: 24 August 2010 / Revised version: 16 February 2011 / Published online: 9 April 2011

Abstract Distributed feedback (DFB) lasing in permanent volume transmission gratings formed in a laser dye-doped organic–inorganic nanocomposite has been investigated. DFB laser cavities were fabricated using one-step two-beam holographic exposure of Pyrromethene 567 (PM567) doped photopolymerizable acrylate monomers containing inorganic ($LaPO_4$) nanoparticles. Compared to the formulation previously utilized, the material composition presented provides longer lifetime of the laser. Spectral and polarization properties, input–output and stability characteristics of the laser output have been investigated by varying the material composition and the patterning parameters. DFB lasing emission of the second and the third diffraction orders has been demonstrated. The spectral linewidth of ∼0.08 nm has been observed at a pump energy threshold of about 0.2 μJ/pulse for the second-order DFB lasing when pumped with 532 nm 500 ps laser pulses. Spectral tuning of the lasing output over ∼56 and ∼7 nm was obtained by varying the grating period and the content of inorganic nanoparticles in the polymer matrix, respectively.

1 Introduction

Distributed feedback dye lasers in which optical feedback is provided due to the Bragg scattering by periodic modulation of gain or/and refractive index (RI, n) of the gain medium were firstly presented by Kogelnik and Shank [1–3]. The interest in DFB lasers became stronger in the last decades; therefore intensive efforts have been dedicated to achieve the incorporation of organic lasing compounds and feedback in solid easy processable organic or organic–inorganic matrices that might replace conventional liquid dye lasers. Lasers based on permanent DFB cavities can be integrated into optical and fluidic microchips usable for medical and bio-applications or chemical point-of-care analysis [4–7]. A number of approaches for fabricating permanent polymer laser cavities based on both surface-relief and volume (refractive index) DFB structures by using organic dyes or semiconductor polymers as gain materials have been proposed [4–27]. In volume DFB lasers the optical feedback can be formed in suitable photoreactive materials by applying UV or holographic lithography. In this case polymers, photopolymers or polymer–liquid crystal composites doped with the active substances like organic laser dyes are exploited [14–22]. A volume optical feedback provides high input/output lasing efficiency (up to 20%), keeping the value of the linewidth of ∼0.01 nm (see, e.g., [15]), and allows introducing polarization modulation into DFB lasers for the optical feedback [23]. Despite variety of approaches for microfabricated polymer-based dye lasers with integrated optical feedback (see the references mentioned before), an intensive search of new materials and approaches to simplify the technology of efficient low-threshold organic DFB-lasers is in progress. In the last years, inorganic nanocrystals have emerged as an attractive new gain medium or as well a material to provide the optical feedback (see, e.g., [27]) for DFB lasers. Semiconductor nanocrystals, quantum dots (CdSe, CdSe/ZnS, PbSe, etc.), homogeneously dispersed in various inorganic matrices, were used mostly as a gain medium with external DFB structures [24–26]. In [27] the stimulated

O.V. Sakhno (✉) · J. Stumpe
Fraunhofer Institute for Applied Polymer Research, Science Campus Golm, Geiselbergstr. 69, 14476 Potsdam, Germany
e-mail: Oksana.Sakhno@iap.fraunhofer.de
Fax: +49-331-5683259

T.N. Smirnova
Institute of Physics NASU, pr. Nauki 46, 03028 Kiev, Ukraine

emission from an organic dye adsorbed within the void network of a one-dimensional photonic crystal, consisting of periodically alternating layers of TiO_2 and SiO_2 nanoparticles, was reported. In all the cases the fabrication technology of the lasing systems is tedious.

Here we report holographic dye-doped photocurable organic–inorganic nanocomposites and a one-step structuring method to fabricate DFB lasers based on a volume distributed feedback. As structuring method for the fabrication of the laser cavities, the holographic photopolymerization was used. UV holographic exposure has been applied directly to the organic–inorganic material consisting of photocurable monomers, inorganic nanoparticles (NPs) and a laser dye. Holographic patterning technique allows fabricating the feedback structures in the gain medium in a single all-optical step by controlling easily their period and geometry. Upon exposure, polymerization in the interference pattern generates a spatial periodic distribution of high RI NPs in low RI polymer matrix, forming a dye-doped refractive index grating. The organic–inorganic nanocomposites proposed provide a higher RI modulation than the neat polymer materials, where the RI modulation originates exclusively from a photoinduced change of the density of polymer matrix. The holographic photocurable nanocomposites doped with inorganic light-emissive nanocrystals and/or organic laser dyes as the suitable materials for producing DFB lasing devices were firstly proposed by us in [28]. DFB lasing action in the dye-doped nanocomposite volume transmission gratings was presented in [29]; more detailed examination of the proposed dye lasers was reported in [30]. As a photostructurable matrix, the organic–inorganic nanocomposite containing ZrO_2 NPs has been previously used. Unfortunately, the ZrO_2 NPs-based organic–inorganic nanocomposite matrix did not provide a long shelf-life of the laser dyes. After one month's storage in the dark a drastic decrease in the photoluminescence (PL) intensity of the doped nanocomposite gratings was observed, which indicates a not complete chemical inertness of the organic–inorganic matrix used with respect to the laser dyes. Chemical reactions between the dye and the organic acid, which was used for modifying ZrO_2 NPs surface to ensure the compatibility of inorganic NPs with organic matrix, have been considered as a possible reason. In this work, in order to provide longer shelf-life of the lasers, the previous material formulation was substituted for another photopolymerizable acrylate-based nanocomposite containing other ($LaPO_4$) inorganic NPs [31]. The diffraction gratings fabricated from this nanocomposite doped with the same laser dye as in [30] perform almost no changes in their optical properties during 12 months' storage and testing. The improved material formulation allowed us to provide comprehensive study of DFB lasing from dye-doped nanocomposite volume gratings. Besides that, the modification of the nanocomposite formulation allowed to improve considerably the output and spectral lasing parameters compared to those presented in [30].

In this work we report a detailed experimental investigation of the lasing performance of optically pumped DFB cavities based on Pyrromethene 567 (PM567) doped polymer-$LaPO_4$ NPs transmission gratings. It has been shown that variation of the composite formulation and the grating periodicity provides an effective optical feedback via both the second and the third Bragg orders and allows controlling the output and spectral performance of laser. The dependence of the lasing performance on the parameters of the material, the efficiency of the feedback and optical pumping are shown and discussed. The approach presented should be interesting for further development of solid-state organic DFB dye laser technology.

2 Experimental

2.1 Material preparation and characterization

The selection of the organic matrix and the development of the holographic organic–inorganic nanocomposite material based on REN-X green NPs (commercial name of $LaPO_4$:Ce^{3+}, Tb^{3+} NPs) have been reported elsewhere [31]. The REN-X green NPs perform low photoactivity, have no absorption in the visible spectral range and posses enough high RI (∼1.85) compared to the RI of the organic matrix used. The NPs form optically transparent dispersion with the concentration up to 35 wt.% in the low-polar acrylate monomer mixture. Despite slightly lower RI, compared to the RI of the ZrO_2 NPs, the REN-X green NPs can provide high enough diffraction efficiency of the final gratings. Moreover, the gratings fabricated from the doped REN-X green NPs based nanocomposites perform almost no changes in their optical properties during storage and testing, which indicates the absence of any chemical reactions between the material components. Besides that, the use of another combination of the acrylate monomers allows obtaining a higher RI of the organic matrix compared to the matrix previously used in [30].

To fabricate the DFB gratings, the mixture of two acrylate monomers—isobornyl acrylate ($n = 1.442$) and pentaerythritol triacrylate ($n = 1.481$) (purchased from Aldrich) in the concentration ratio of 8:2 was used as organic matrix material. The acrylates were not purified before use. The acrylate monomer mixture contains a small amount (1.5 wt.%) of the UV-photoinitiator Irgacure 1700 (Ciba Specialty Chemicals) to provide the free radicals for initiating photopolymerization by UV light (364 nm). The REN-X green NPs (purchased from Nanosolutions GmbH, average diameter is of ∼6 nm) were employed as an inorganic high-RI part of the nanocomposite. The content

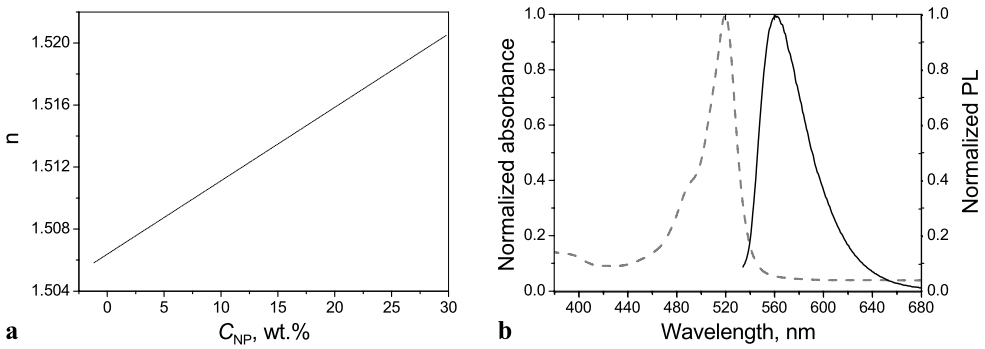

Fig. 1 (**a**) RI of the nanocomposite as a function of the NP content; (**b**) absorption (*dash line*), and the PL (*solid line*) spectrum of the doped nanocomposite floodlight exposed film (thickness of the film—12 μm)

of the NPs (C_{NP}) in the nanocomposite was varied in the range of 10–27 wt.%, which allows fine tuning of the RI of the material from ∼1.505 at $C_{NP} = 10$ wt.% to ∼1.52 at $C_{NP} = 27$ wt.%. The dependence of the RI of the material as a function of C_{NP} is shown in Fig. 1a. In order to provide the emissive properties of the DFB gratings, the active laser substance should be incorporated into the nanocomposite. Three often usable commercial lasing dyes, Rhodamin 6G, PM567 and DCM (4-dicyanomethylene-2-methyl-6-P-dimethylaminostyryl-4H-pyran), have been tested. According to several specific requirements, like photostability for the exposure to UV light (upon holographic recording of the grating), good solubility in the initial nanocomposite and efficiency of the lasing emission from the resulting DFB cavities, PM567 (Exciton, Inc.) laser dye was selected as the most suitable for the material formulation used. Moreover, high quantum fluorescence yield, high photostability and good lasing performance of pyrromethene dyes when incorporated into solid hosts are well known from the literature [32 and the references therein]. The dye (0.4–1.5 wt.%) was dissolved firstly in the monomer blend containing the photoinitiator. After addition of the dispersion of the NPs in pentane and evaporation of solvent, the doped organic–inorganic nanocomposites were used for the recording of gain gratings.

The RI of the monomers and the nanocomposites were measured using Abbe refractometer (Carl Zeiss, Jena). Absorption and PL spectrum were measured with Perkin-Elmer UV-vis and PL spectrometers. The samples were prepared by sandwiching a drop of the nanocomposite between two glass substrates having RI n_s ∼1.514 (at 633 nm). The thickness of the film (d) was controlled by Teflon spacers of the thickness 10 and 12 μm.

In Fig. 1b, the absorption (dash line) and the PL (solid line) spectra of the film prepared from the PM567-doped nanocomposite containing 27 wt.% of the NPs are shown. The luminescence maximum is located around 562 nm (spectral width at half-maximum is ∼42 nm).

2.2 Holographic fabrication of DFB structures and lasing measurements

DFB transmission gratings were recorded by exposing the films of the doped organic–inorganic nanocomposite to the interference pattern formed by two s-polarized laser beams (Ar-ion (Ar^+) laser, $\lambda_r = 364$ nm, intensity $I \approx 5$ mW/cm^2 per beam). The spatial period of the grating (Λ) was controlled by the angle between the recording beams. The grating formation was monitored in real time by diffraction of a He-Ne laser beam (s-polarization, $\lambda_t = 632.8$ nm). UV floodlight exposure of the sample with a UV-lamp after holographic inscription was performed to provide curing of residual monomers in the film area around the grating. The diffraction efficiency (η) of the grating was determined as $\eta = I_{dif}/(I_{tr} + I_{dif})$, where I_{tr} and I_{dif} are the intensity of 0th diffraction order (transmitted beam) and −1st diffraction order (diffracted beam), respectively. The RI modulation amplitude of the grating (n_1) was estimated using the experimental values of η according to the Kogelnik formula [33]: $n_1 = (\lambda_t \cdot \cos\theta_B \cdot \arcsin\sqrt{\eta})/(\pi \cdot d)$, where θ_B is the Bragg angle within the material. The values of n_1 were measured at the readout wavelength $\lambda_t = 632.8$ nm.

For optical pumping of the doped DFB gratings a Q-switched frequency doubled Nd:YAG pulsed laser (Soliton) operating at 532 nm (pulse width 500 ps, repetition rate $\nu = 10$ or 100 Hz, maximum pulse energy $E_p = 30$ μJ, linear (vertical) polarization) was used in the lasing experiments. The output pulse energy of the pump beam was controlled using neutral density filters. The energies from the pump and the nanocomposite lasers were measured using laser power/energy meter (Coherent, LabMax). Cylindrical lens was used in order to shape the pump beam into a narrow stripe of ∼4 mm length and ∼0.5 mm width. The light stripe was oriented along the grating vector. $\vec{E}$ of the pump light is oriented parallel to the grating planes (s-polarization, correspondently). A condenser lens was used to collect light from the edge of the sample in an optical fibre coupled to a charge-coupled device spectrometer Jobin Ivon (the wavelength resolutions of the monochromator are 0.7 and 0.07 nm). After holographic and flood-

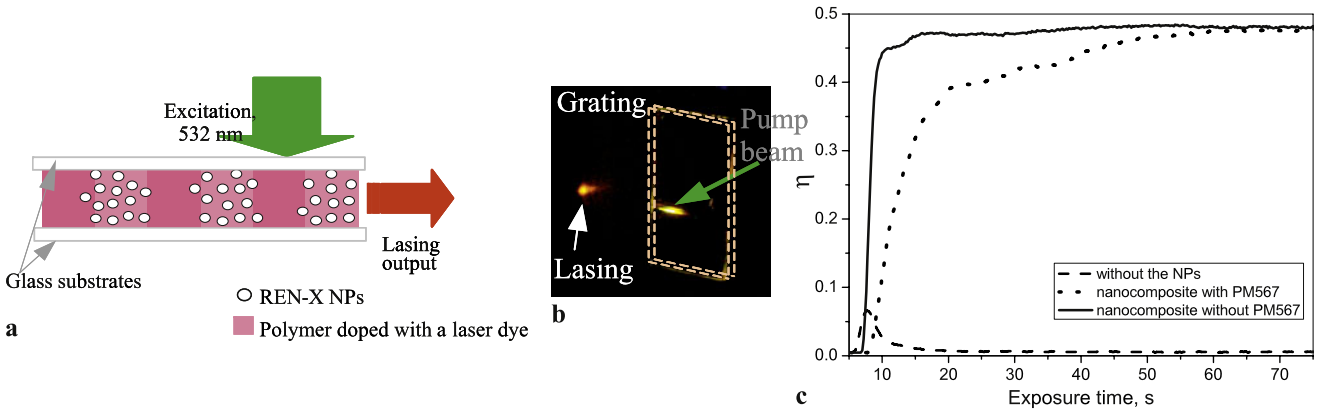

Fig. 2 (**a**) Schematic description of the distribution of the material components in a dye-doped nanocomposite DFB grating, the scheme of optical pumping and direction of the lasing output; (**b**) the image of the nanocomposite DFB laser operation; (**c**) diffraction efficiency of the grating as a function of exposure time in the material without the NPs (*black dash line*), in the nanocomposite with 27 wt.% of the NPs (*black solid line*) and in the nanocomposite with 27 wt.% of the NPs doped with 0.7 wt.% of PM567 (*gray dash line*) ($d = 10$ μm, $\Lambda = 450$ nm, starting time of holographic exposure 5 s)

light exposure, the DFB-triplex lasing structures (substrate-DFB grating-substrate) were tested with respect to the lasing performance. The transversal pumping scheme used allows achieving a long gain medium and providing effective distributed feedback even at low n_1. The grating planes are perpendicular to the substrate and the laser emission comes out from the edge of the film, perpendicularly to the grating fringes. Schematic presentations of the nanocomposite grating-based DFB laser and the pumping scheme used in the experiments are shown in Fig. 2a.

3 Results and discussion

3.1 DFB lasing in nanocomposite gratings

The holographic properties of the photopolymerizable organic–inorganic composites containing REN-X green NPs, the mechanism of the grating formation as well as the parameters of the volume nanocomposite gratings have been reported in [31]. It was shown that the nanocomposite containing 27 wt.% of the NPs results in the RI modulation amplitude (n_1) up to ~0.011 in the range of the grating periodicities of $\Lambda = 0.45$–1.5 μm. The interference exposure causes the initiation of free radicals from the photoinitiator, which triggers a fast photopolymerization of the multifunctional monomer in the bright regions of the interference pattern. The formed polymer network causes segregation of less reactive monomer and the NPs, driving them to the non-cross-linked dark regions of the film. After complete consumption of the active monomers, a permanent periodic distribution of high RI NPs in low RI polymer matrix is formed. The difference of the RI of the material in the NP-rich and the NP-poor areas provides the RI modulation of the resulting nanocomposite gratings and, correspondingly, optical distributed feedback. In Fig. 2 the typical time-evolutions of η of the gratings with $\Lambda = 450$ nm in the REN-X green NPs nanocomposite without the laser dye, in the nanocomposite doped with PM567, and in the basic monomer mixture without the NPs are shown. The addition of the dye in the material increases the induction period of the grating formation for several seconds and changes slightly the shape of the kinetics curve. The final values of η as well as optical quality of the gratings, inscribed in the non-doped and doped materials, differ just slightly (Fig. 2b). Almost no degradation of the absorption of PM567-doped films (~5%) was observed during typical holographic patterning process.

According to DFB laser theory [1], for mth-order operation, the wavelength of dye laser (λ_{las}) is given by $\lambda_{las} = 2n_{eff}\Lambda/m$, where n_{eff} is the effective index of material at the lasing wavelength. Supposing that distributed feedback in our DFB lasing system is provided via the second-order Bragg reflection induced by the RI modulation ($m = 2$) and in order to obtain the lasing emission in 560–630 nm spectral region (according to the PL spectrum of PM567 in the nanocomposite, Fig. 1b), an appropriate period of DFB gratings (Λ) was selected in the range of 370–420 nm. To obtain lasing via the third Bragg order, Λ should be in the range of 560–620 nm. The RI of the nanocomposite film containing 27 wt.% of the REN-X green NPs ($n \approx 1.518$) was used as n_{eff} for the estimations.

In the doped nanocomposite grating, composed of the polymer matrix, inorganic NPs and a laser dye, the optical feedback should be provided by the spatial modulation of the concentration of the NPs (C_{NP}) (phase grating) and of a gain (C_{LD}) (amplitude grating) (Fig. 2a). At that, both subgratings are shifted half a period (π) with respect to each other, since the high-RI NPs are located mostly in the

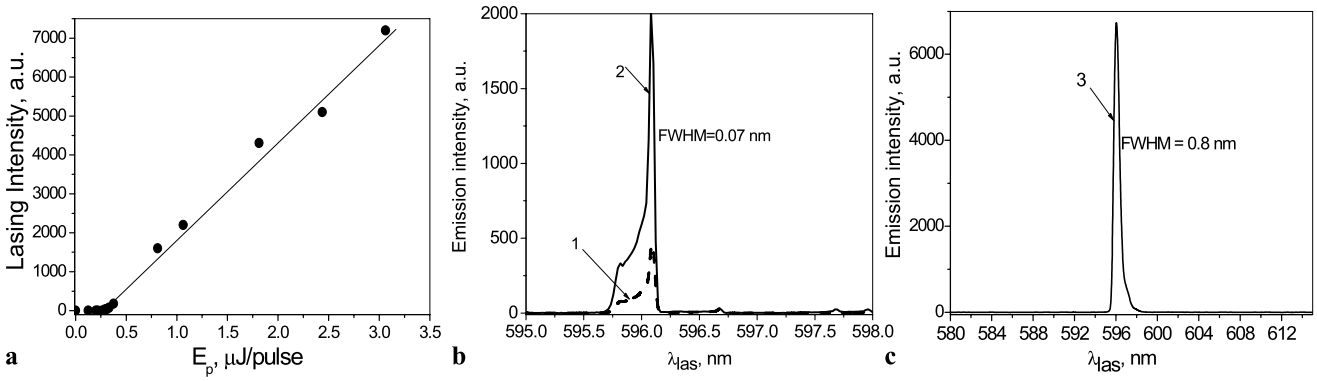

Fig. 3 (**a**) The output intensity as a function of the 532 nm laser pump energy; (**b**) the lasing spectra at different pump energy: *1* E_p = 0.35 μJ/pulse; *2* E_p = 1.25 μJ/pulse; *3* E_p = 3 μJ/pulse (the intensity of the *curve 1* is multiplied by 10). Parameters of the grating: $\Lambda = 392$ nm, $d = 12$ μm, optical density of the film at $\lambda = 532$ nm $OD = 0.5$, $n_1 \cong 0.0075$

fringes of the grating, corresponding to the regions of the destructive interference, and the dye molecules should be located mostly in the fringes, corresponding to the regions of the constructive interference. According to the theoretical conclusions of [34], the light amplification in volume DFB lasers operating by the second diffraction order is more favorable at "out-of-phase" matching (this configuration is realized in the doped nanocomposite gratings) than at "in-phase matching," when the phases of both the gratings coincide. It makes the doped nanocomposite gratings a good candidate for efficient lasing devices.

The laser devices under study work well (showing the lowest lasing threshold and the narrowest width of the lasing line) if the pump stripe is well oriented perpendicularly to the grating fringes. The lasing operation of the DFB nanocomposite grating doped with PM567 and emitted at $\lambda_{las} = 596$ nm is shown in Fig. 2b. The measured output characteristics of the doped grating, emitted at 596 nm, are shown in Fig. 3a, b. The yielding input–output dependence performs at a pronounced threshold behavior, typical for the progress of DFB lasing. The lowest pump energy threshold was found to be about 0.25 μJ/pulse (∼12.5 μJ/cm^2) in this case (Fig. 3a). Above the lasing threshold the output lasing intensity increases almost linearly with increasing pump laser energy (Fig. 3a).

The lasing spectra measured at different pump energies are shown in Fig. 3b. The spectrum shape is typical for the laser systems under study. Near the threshold energy a sharp peak with a full width of half-maximum (FWHM) of ∼0.1 nm and a short-wavelength shoulder is observed. The shape of the spectrum is not changed upon the growth of pump energy up to ∼1.25 μJ/pulse (a 5-fold excess of the lasing threshold). However, as the pumping is gradually increased, high-order modes (having higher threshold energies) begin to oscillate. At pump energies > 1.3 μJ/pulse, the output emission becomes multimode which causes a widening of the emission spectrum. The FWHM increases to ∼1 nm and remains constant up to pump energy which is 10-fold higher than the corresponding pump threshold. It should be noted that depending on the grating thickness and the pumping conditions, FWHM can increase up to ∼2 nm. It is known [see, e.g., 2, 35, 36] that it is difficult to achieve stable single-mode emission from DFB lasers based on periodical modulation of the RI of the active medium. DFB cavity based on phase grating provides the propagation of at least two lasing modes with a low threshold, situated at both band edges of the Bragg resonance. Usually the number of the lasing modes increases with pump intensity.

The second-order output lasing energy from the doped grating having $d = 20$ μm was measured to be about 1.4 μJ/pulse at pump energy of 17 μJ/pulse, giving the pump-to-laser conversion efficiency of ∼8%, which is comparable with the conversion slope efficiency (∼6.8%) for the two-dimensional DFB laser based on the conjugated polymer [13].

3.2 Polarization, laser threshold and spectral tunability of lasing output

The dependence of polarization and intensity of the emitted laser light on the polarization of the pumping light has been investigated by inserting a polarizer (λ/2 plate) and an analyzer in the measurement scheme. The measurements were carried out for both *s*- and *p*-polarizations of the pump light at pump energy of ∼1.2 μJ/pulse. The experimental results are shown in Fig. 4. It was found that the lasing emission is almost completely *s*-polarized with a degree of polarization of about 95% when the samples were pumped with *s*-polarized light. The degree of polarization was defined as $(I_{las}^{II} - I_{las}^{\perp})/(I_{las}^{II} + I_{las}^{\perp})$, where I_{las}^{II}, $I_{las}^{\perp}$ are the intensities of the lasing emission if the analyzer is oriented parallel and perpendicular to $\vec{E}$ of the pump beam, respectively. When pumped with *p*-polarized light (with the same pump energy), the intensity of the output emission decreases suffi-

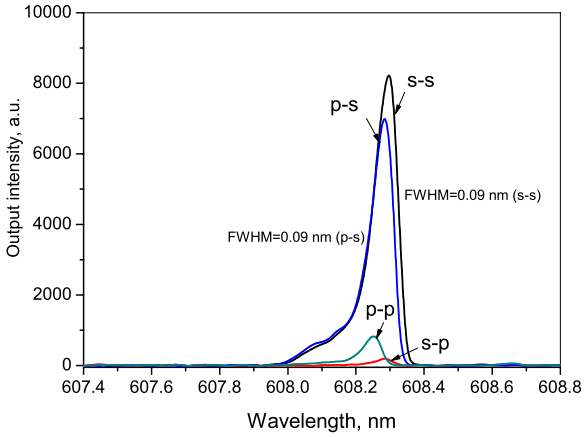

Fig. 4 DFB laser output spectra for s- and p-polarized pumping; polarization directions of the pump light and the output emission are indicated

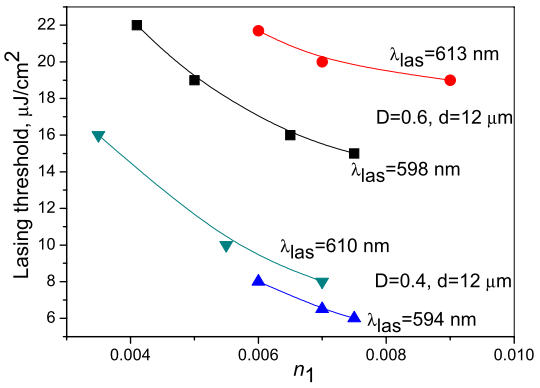

Fig. 5 Lasing threshold as a function of the RI contrast (n_1) for the gratings with different periodicity and concentration of the laser dye ($d = 12$ μm)

ciently. Both the s- and p-polarized components exist in the output signal. At that, the intensity of the s-component was found to be about 10 times higher than the intensity of the p-component. The data obtained are in agreement with the polarization parameters of DFB waveguide lasers with multiwavelength output (see, e.g., [37]). Since the thickness of the active layer of the system under study is of about 10 μm, the output emission is multimode. At that, the number of laser modes is determined by different factors like thickness and the RI of the waveguide and the substrates, energy and polarization state of the pump light. For instance, it was shown that 8 pairs of TE/TM (s- and p-polarized) modes exist in the film of $n = 1.55$ and thickness of 6.7 μm, deposited on glass substrate of $n_s = 1.51$ [37]. We should note that the TM modes are usually blue-shifted concerning to the spectral position of the TE modes [37]. According to our results, the last effect becomes apparent in the short-wavelength shift of the p-polarized laser lines. The decrease in the output laser intensity with a p-polarized pump has probably the same origin as that in the dye lasers with a transversal pumping, those performing a gain dichroism [38]. Upon the excitation of chaotically distributed dye-dipoles by the light having $\vec{E}$ perpendicular to the axis of resonator, the maximum emission will coincide with the axis of resonator and gained efficiently. In the case of $\vec{E}$ parallel to the axis of resonator, the situation will be opposite and the intensity of lasing will decrease. This effect increases especially in the solid solutions of the dyes, where the time of rotational relaxation of active molecules decreases considerably [39, 40]. Besides that, the lasing efficiency will be affected by specific interactions of s- and p-polarized emission of dye molecules with both the RI and gain gratings [39]. The glass–DFB grating–glass layers constitute plane symmetric couples' waveguides that can support an increasing number of propagating modes in thick enough (10–20 μm) volume grating. Since lasers with the multiwavelength output have found applications as sensors for environmental monitoring or as light sources in wavelength division multiplexing networks, the detailed investigation of multimode emission of nanocomposite DFB dye lasers will be studied further.

The threshold parameters of the lasers depend on the efficiency and the period of DFB cavity, as well as on the concentration of the laser dye in the material. The results obtained are shown in Fig. 5. The measurements have been carried out with an s-polarized pump beam. The efficiency of the DFB cavity upon transverse pumping is determined by the reflectivity of the grating in the second diffraction order. Besides that, the first-order diffraction by the second harmonic of the RI modulation, n_2 (which cannot be measured experimentally for the gratings with small periods), can contribute sufficiently to the reflectivity as well. The estimations of the contribution of n_2 to the efficiency of the ZrO_2 NPs-based DFB laser cavity [30] have shown that even a small RI contrast (n_2) can provide high reflectivity of the grating ($\eta^{\text{refl}} = 0.6$–0.9), which, in turn, can ensure an effective optical feedback.

The lasing threshold decreases with increasing n_1, which indicates a higher reflectivity of the DFB grating (Fig. 5). At the same time, the lasing threshold changes slowly with increasing n_1, which is probably related to the saturation of η of the reflection grating providing feedback. Decreasing C_{LD} to its optimized value, at which the optical density (OD) of the film at the wavelength of optical pumping is in the range of 0.4–0.6, causes a decrease in the lasing threshold. This observation is in good agreement with the results reported in [30].

The lasing threshold increases with Λ and, correspondingly, with increasing λ_{las} from 594 to 615 nm (measured for the gratings with comparable n_1 and OD). The latter can be related to the fact that the lasing wavelengths longer than 600 nm correspond to a long-wavelength part of the gain spectrum, where the gain efficiency decreases. On the other hand, the lasing threshold increases as the emission is being

Table 1 Spectral tunability (λ_{las}) of the nanocomposite DFB dye laser: dependence on the grating period (Λ), concentration of the NPs (C_{NP}) and the diffraction order (m)

m	C_{NP}, wt.%	Λ, nm	λ_{las}, nm
2	27	375	568
2	27	383	585
2	27	392	596
2	27	394	598
2	27	410	625
2	10	394	591
2	10	410	619
3	27	559	567
3	27	586	585

tuned toward the blue edge of the tuning range. For the limit case of $\lambda_{las} = 568$ nm, the laser threshold increases sufficiently (up to ~2 μJ/pulse) compared to the value measured for $\lambda_{las} = 594$ nm, ~0.12 μJ/pulse ($OD = 0.4$; these data are not shown in Fig. 5). The observed behavior can be explained that as the emission wavelength approaches the edge of the gain spectrum the oscillating light experiences less gain per one feedback cycle, while at the same time the self-absorption losses become larger [41]. Thus, the optical gain of the nanocomposite DFB cavities doped with the dye of the concentration mentioned above is maximal in the spectral range of 580–590 nm. Therefore, at the optimized parameters of the feedback structure ($OD(532\text{ nm}) \cong 0.45, n_1 \cong 0.008, d = 12$ μm), the nanocomposite DFB lasers exhibit the pump threshold in the range of 6–8 μJ/cm^2 (0.12–0.16 μJ/pulse) with an FWHM of about 0.1 nm over 594–610 nm spectral range (at pump energy of ≤ 5-fold higher than the threshold value).

The lasing wavelength can be varied by changing either Λ of the DFB grating or C_{NP} (i.e. n_{eff}). To examine the spectral tunability of nanocomposite dye lasers, a range of gratings with variable periodicity have been fabricated. The nanocomposites containing 27 and 10 wt.% NPs doped with 0.7 wt.% of PM567 ($OD \approx 0.5$) were exploited. The measured laser wavelengths (λ_{las}) and the corresponding Λ are collected in Table 1. Depending on the grating period, the laser spectral output could be tuned at about 60 nm, which is over almost entire emission spectrum of PM567. The change of λ_{las} as large as ~5–7 nm was observed by decreasing the NP concentration in polymer from $C_{NP} = 27$ to 10 wt.% (n_{eff} was changed from ~1.52 to ~1.505, respectively). With the decrease of C_{NP}, the lasing wavelength showed a blue shift. The corresponding values of λ_{las} obtained for two grating periods are also shown in Table 1. The lasing threshold decreases with increasing C_{NP}: from ~0.7 μJ/pulse (35 μJ/cm^2) for the grating with $C_{NP} = 10$ wt.% and $n_1 = 0.0055$ to ~0.25 μJ/pulse (12.5 μJ/cm^2) for the grating with $C_{NP} = 27$ wt.% and $n_1 = 0.0096$, probably due to a lower efficiency of the resonant feedback (i.e. n_1) in the material with $C_{NP} = 10$ wt.%.

DFB lasing at higher reflection order ($m = 3$) has been obtained as well by using the gratings with $\Lambda > 550$ nm (Table 1). The lasing threshold in this case was higher (~1.1–1.4 μJ/pulse) in comparison with the second-order cavities fabricated from the same material and operated in the same spectral range. The latter is explained by even lower value of the RI modulation for higher diffraction orders. We suppose that in this case the first-order diffraction by the third harmonic of the RI, n_3, provides the main contribution to the reflectivity of the grating. The third harmonic of the RI appears due to the nonlinearity of the material response to the interference pattern.

3.3 Stability of DFB lasing

Degradation of dye molecules in solid-state hosts leads to a reduction of laser output power and has been a crucial bottleneck for utilization of dye organic solid-state lasers [42–44]. Therefore the improvement of the stability of polymer dye lasers to obtain high operation lifetime of lasers is a subject of interest. Recently, an Nd:YAG pumped DFB polymer dye laser showed threshold energy density of 45 μJ/cm^2 and a relatively long lifetime of ~3×10^5 shots [45]. The PM567-doped plastic waveguide with prefabricated DFB structures pumped by a Nd:YAG microchip laser demonstrated a threshold of about 42 μJ/cm^2 and lifetime of ~4.5×10^5 shots at pump energy density of about 10^3 μJ/cm^2 [46].

Stability performance of the nanocomposite DFB lasers has been examined at different pump energies and repetition rates at room (air) conditions. The measurements were performed by observing the output energy (in a.u.) via the number of excitation shots. The lifetime is determined as a number of shots corresponding to decrease in the laser output down to half of its initial value. The results are displayed in Fig. 6a, b.

To determine the photostability of PM567 in dye-doped inorganically non-modified and modified acrylate matrices, the time evolution of amplified spontaneous emission from dye-doped films ($d = 10$ μm) prepared from the pure polymer and polymer-NPs materials has been investigated (Fig. 6a). The films were pumped with $\nu = 100$ Hz 532 nm pulses of ~4 μJ pump energy (200 μJ/cm^2). We have not observed a considerable difference in the stabilities of the films without and with the NPs of different concentrations. All films showed the 50% output decrease after approximately 2.2×10^4 shots. Such small difference is, probably, related to a low photoactivity and a low volume fraction of inorganic additives in the organic matrix (26 wt.% of the REN-X green NPs is equal to ~5 vol.% [31]). It seems that the content of the NPs in the composite is sufficient to provide an effective distributed feedback but it does not change enough the

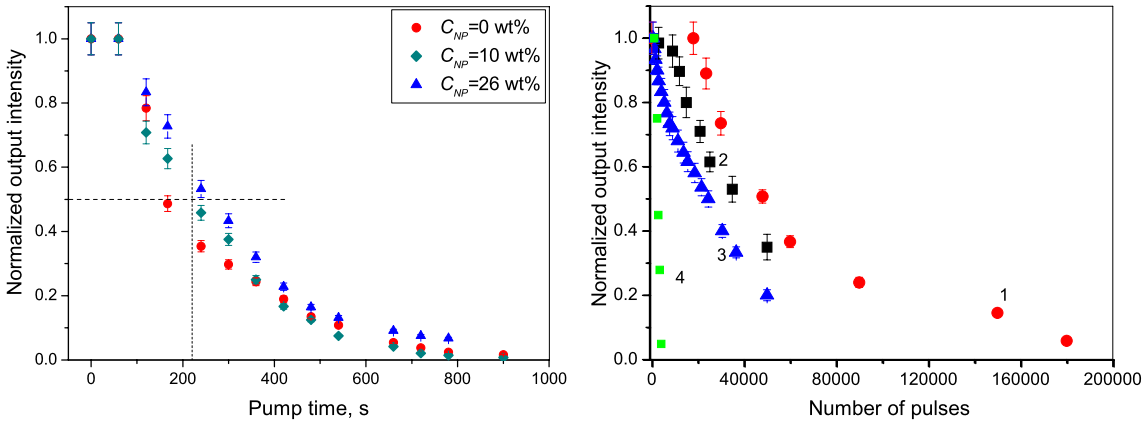

Fig. 6 (**a**) Stability of the dye-doped films with different content of the NPs (C_{NP}), $\nu = 100$ Hz repetition rate, $E_p = 4$ μJ/pulse; (**b**) degradation of the laser output of the gratings doped with PM567 (*1–3*) at different pump repetition rates and pulse energy: $\nu = 100$ Hz, $E_p = 2$ μJ/pulse (*1*); $\nu = 10$ Hz, $E_p = 2$ μJ/pulse (*2*); $\nu = 10$ Hz, $E_p = 4$ μJ/pulse (*3*) and doped with DCM (*4*) at $\nu = 10$ Hz, $E_p = 20$ μJ/pulse

viscoelastic properties of polymer matrix and, in turn, the lifetime of the laser dye.

Figure 6b displays the evolution of a normalized output power as a function of the number of pump pulses for the PM567-doped DFB grating ($OD(532\text{ nm}) = 0.5$). The experiments were carried out at 10 and 100 Hz repetition rates with pump energies of 2 μJ/pulse (100 μJ/cm^2) and 4 μJ/pulse (20 μJ/cm^2), respectively, that is approximately 10 and 20 times higher than the lasing threshold. It is seen from the results that increasing the pulse rate at constant pump energy does not change the operation lifetime of the nanocomposite laser, which is in agreement with the data of [43, 46]. In both cases the operation lifetime was found to be about 4×10^4 shots (~1 h and ~7 min of the laser operation at $\nu = 10$ and 100 Hz, respectively). It indicates that under the repetition rates applied, the effect of heating of the host polymeric matrix does not play a substantial role in the stimulation of photodecomposition of the dye. Twice increasing pump energy at 10 Hz repetition rate causes a decrease in the operation lifetime to 2.4×10^4 shots. Thus, a low lasing threshold of the laser devices is favorable to obtain longer operation lifetime. For the comparison, the same test was done for the grating doped with the same concentration of DCM laser dye. The stability of the grating doped with DCM was found to be much lower, $\sim 2 \times 10^3$ shots at pump energy of 20 μJ/pulse (approximately 3 times higher than the corresponding lasing threshold (~6 μJ/pulse)).

It is known that the photostability of PM567 in solution and in solid polymers strongly depends on the presence of oxygen [32, 42, 47, 48]. The most probable photodegradation mechanism could be attributed to self- and radical-sensitized photo-oxidation, i.e., singlet-state oxygen molecules sensitized by other species, such as triplet-state PM567 molecules or free radicals, should be responsible for the permanent degradation of PM567 dye and decreasing laser output in most cases. To obtain higher photostability of PM567, antioxidant additives acting as singlet-state quencher or free-radical scavenger have to be added into host matrix together with PM567 [42, 47–50]. It should be noted that the photostability data of the nanocomposite DFB dye laser presented have been obtained for the systems to which any special methods to improve the stability, like purification of the material components, addition of functional additives, removal of oxygen from the initial nanocomposite, capsulation of the DFB triplex, have not been applied. On the other hand, it is difficult to compare the data received because of the absence of the similar systems data in the literature. The optimization of the nanocomposite formulation and the laser fabrication procedure in order to increase the laser operating time is in progress.

In summary, fabrication and characterization of DFB dye lasers based on doped solid-state volume Bragg gratings have been presented. The improved organic–inorganic nanocomposite doped with Pyrromethene 567 laser dye has been used as an active medium for photoinduced DFB lasers. Permanent DFB laser cavities have been fabricated using one-step holographic photopolymerization of the composite materials containing acrylate monomers, photoinitiator, high-RI inorganic nanoparticles and a laser dye. We have shown that the lasing threshold depends on the efficiency of the DFB grating (RI modulation amplitude), period of the grating (position of the lasing wavelength in respect to the gain band of the laser dye) and the concentration of the laser dye. By optimizing the material and the feedback structure, a narrow linewidth oscillation with the threshold pump energy of ~0.2 and of ~1.1 μJ/pulse was achieved for the second and the third Bragg orders lasing, respectively. The wide-band tuning of the DFB laser output from 568 to 625 nm has been demonstrated for the second-order action due to the variation of the grating period. By changing the NP concentration in the polymer matrix the lasing

wavelength can be shifted over ∼7 nm. Peak pump/output conversion efficiency of about 8% has been achieved at an operating wavelength of 594 nm. It was found that the output emission is *s*-polarized with a polarization contrast as large as 0.95 when the pump light is *s*-polarized. Both *s*- and *p*-polarized lasing modes exist in the output emission at *p*-polarized pumping: the intensity of the *s*-component is about 10 times higher than the intensity of the *p*-component. The PM567-doped nanocomposite matrix provides the stability of the laser emission of $\sim 4 \times 10^4$ shots at 10 Hz repetition rate at pump energy of 10 times higher than the lasing threshold value. The laser material will be optimized in respect to a longer operation time. Further study will be focused on the investigation of the lasing modes and on the development of the theory describing light amplification in this kind of laser cavities. Altogether, the results presented in this work indicate that holographically photostructurable materials open the way to a one-step fabrication process of effective and cheap tunable solid-state lasers based on dye-doped organic–inorganic host systems.

Acknowledgements The work was supported by the Fraunhofer Society, Germany, and by the grant of the Target Comprehensive Program of Fundamental Research of National Academy of Science of Ukraine "Fundamental Problems of Nanostructured Systems, Nanomaterials, and Nanotechnologies." The authors gratefully thank T. Rabe for providing the setup for the lasing experiments and N. Hildebrandt for the support of the work.

References

1. H. Kogelnik, C.V. Shank, Appl. Phys. Lett. **18**, 152 (1971)
2. C.V. Shank, J.E. Bjorkholm, H. Kogelnik, Appl. Phys. Lett. **18**, 395 (1971)
3. H. Kogelnik, C.V. Shank, Appl. Phys. **43**, 2327 (1972)
4. D. Schneider, T. Rabe, Th. Riedl, Th. Dobbeling, M. Kröger, E. Becker, H.H. Johannes, W. Kowalsky, Th. Weinmann, J. Wang, P. Hitze, A. Gerhard, Ph. Stössel, H. Vestweber, Adv. Mater. **17**, 31 (2005)
5. Y. Oki, Sh. Miyamoto, M. Maeda, Opt. Lett. **27**, 1220 (2002)
6. Ch. Vannahme, S. Klinkhammer, F. Brinkmann, S. Lenhert, T. Griossmann, U. Lemmer, T. Mappes, Proc. SPIE **7715**, 77151H (2010)
7. M. Lu, S.S. Gjoi, C.J. Wagner, J.G. Eden, B.T. Cunningham, Appl. Phys. Lett. **92**, 261502 (2008)
8. K. Yamashita, M. Arimatsu, M. Takayama, K. Oe, H. Yanagi, Appl. Phys. Lett. **92**, 243306 (2008)
9. E. Mele, A. Camposeo, R. Stabile, P. Del Carro, F. Di Benedetto, L. Persano, R. Cingolani, D. Pisigano, Appl. Phys. Lett. **89**, 131109 (2006)
10. S. Baslev, T. Rasmusse, P. Shi, A. Kristen, J. Micromech. Microeng. **15**, 2456 (2005)
11. C. Karnutsch, C. Gyrtner, V. Haug, U. Lemmer, T. Farrel, B.S. Nehls, U. Scherf, J. Wang, T. Weinmann, G. Heliotis, C. Pflumm, J.C. deMello, D.D.C. Bradly, Appl. Phys. Lett. **89**, 201108 (2006)
12. S. Klinkhammer, T. Woggon, U. Geyer, C. Vannahme, S. Dehm, T. Mappes, U. Lemmer, Appl. Phys. B **97**, 787 (2009)
13. G.A. Turnbull, P. Andreew, W.L. Barnes, I.D.W. Samuel, Appl. Phys. Lett. **82**, 313 (2003)
14. M. Nagawa, M. Ichikawa, T. Koyama, H. Shirai, Y. Taniguchia, A. Hongo, Sh. Tsuji, Y. Nakano, Appl. Phys. Lett. **77**, 2641 (2000)
15. T.Sh. Efendiev, V.M. Katarkevich, A.N. Rubinov, V.A. Zaporozhchenko, in *Proc. 15th Belar.–Lithuan. Sem. Las. Opt. Nonlin*. Minsk (2000), p. 150
16. G. Kranzelbinder, E. Tousssaere, J. Zyss, A. Pogantsch, E.W.J. List, H. Tillman, H.H. Horhold, Appl. Phys. Lett. **80**, 716 (2002)
17. Y. Oki, T. Yoshiura, Y. Chisaki, M. Maeda, Appl. Opt. **41**, 5030 (2002)
18. G.A. Turnbull, T.F. Krauss, W.L. Barnes, I.D.W. Samuel, Synth. Met. **121**, 1757 (2001)
19. V.K. Hsiao, Ch. Lu, G.S. He, M. Pan, A.N. Cartwrite, P.N. Prasad, R. Jakubiak, R.A. Vaia, T.J. Bunning, Opt. Express **13**, 3787 (2005)
20. R. Jakubiak, T.J. Bunning, R.A. Vaia, L.V. Natarajan, V.P. Tondiglia, Adv. Mater. **15**, 241 (2003)
21. T. Kavc, G. Langer, W. Kern, G. Kranzelbinder, E. Toussaere, G.A. Turnbull, I.D.W. Samuel, K.F. Iskra, T. Neger, A. Pogantsch, Chem. Mater. **14**, 4178 (2002)
22. D.C. Oliveira, K. Messaddeq, K. Dahmouche, S.I.J. Ribeiro, R.R. Goncalves, A. Vesperini, D. Gindre, J.M. Nunzi, J. Sol-Gel Sci. Technol. **40**, 358 (2006)
23. F. Chen, D. Gindre, J.-M. Nunzi, Opt. Express **16**, 16746 (2008)
24. V.C. Sundar Eisler, M.G. Bawendi, M. Walsh, H.J. Smith, V.I. Klimov, Appl. Phys. Lett. **80**, 4614 (2002)
25. V.C. Sundar, H.-J. Eisler, T. Deng, E.L. Thomas, Yi. Chan, M.G. Bawendi, Adv. Mater. **16**, 2137 (2004)
26. Y. Chan, J.-V. Caruge, P.T. Snee, M.G. Bawendi, Appl. Phys. Lett. **85**, 2460 (2004)
27. F. Scotognella, D.P. Puzzo, A. Monguzzi, D.S. Wiersma, D. Maschke, R. Tubino, G.A. Ozin, Small **5**, 2048 (2009)
28. T.N. Smirnova, O.V. Sakhno, P.V. Yezhov, L.M. Kokhtych, L.M. Goldenberg, J. Stumpe, Nanotechnology **20**, 245707 (2009)
29. O.V. Sakhno, L.M. Goldenberg, T.N. Smirnova, J. Stumpe, Proc. SPIE **7487**, 7487H1 (2009)
30. T.N. Smirnova, O.V. Sakhno, J. Stumpe, V. Kzianzou, S. Schrader, J. Opt. **11**, 035709 (2011)
31. O.V. Sakhno, T.N. Smirnova, L.M. Goldenberg, J. Stumpe, Mater. Sci. Eng., C, Biomim. Mater., Sens. Syst. **28**, 28 (2008)
32. A. Costela, I. Garsia-Moreno, C. Gomez, F. Amat-Guerri, M. Liras, R. Sastre, Appl. Phys. B **76**, 365 (2003)
33. H. Kogelnik, Bell Syst. Tech. J. **48**, 2909 (1969)
34. M.V. Vasnetsov, Y.V. Bazhenov, S.S. Slussarenko, G. Abbate, J. Opt. Soc. Am. B **26**, 1975(2009)
35. R.G. Hunsperger, *Integrated Optics: Theory and Technology* (Springer, Berlin, Heidelberg, New York, Tokyo, 1984)
36. A. Yariv, P. Yen, *Optical Waves in Crystals: Propagation and Control of Laser Radiation* (Wiley, New York, 1984)
37. Ch. Ye, L. Shi, J. Wang, D. Loa, X.-L. Zhu, Appl. Phys. Lett. **83**, 4101 (2003)
38. F.P. Schaefer (ed.) *Dye Lasers* (Springer, Berlin-Heidelberg-New York, 1973)
39. D. Wright, E. Brasselet, J. Zyss, G. Langer, W. Kern, J. Opt. Soc. Am. B **21**, 944 (2004)
40. V.I. Bezrodnyj, E.A. Tikhonov, Ukr. Phys. J. **27**, 1113 (1982)
41. G. Heliotis, R. Xia, D.D.C. Bradley, G.A. Turnbull, I.D.W. Samuel, P. Andreew, W.L. Barnes, J. Appl. Phys. **96**, 6959 (2004)
42. K.M. Dymaev, A.A. Manenkov, A.P. Maslyukov, G.A. Matyushin, V.S. Nechitailo, A.M. Prokhorov, J. Opt. Soc. Am. B **9**, 134 (1992)
43. R. Sastre, A. Costela, Adv. Mater. **7**, 198 (1995)
44. A. Costela, I. Garsia-Moreno, C. Gomez, O. Garsia, R. Sastre, Chem. Phys. Lett. **369**, 656 (2003)

45. M.D. Rahn, T.A. King, Appl. Opt. **34**, 8260 (1995)
46. T. Voss, D. Scheel, W. Schade, Appl. Phys. B **73**, 105 (2001)
47. Y. Oki, Sh. Miyamoto, M. Tanaka, D. Zuo, M. Maeda, Opt. Commun. **214**, 277 (2002)
48. Y. Yang, G. Qian, D. Su, M. Wang, Opt. Commun. **239**, 415 (2004)
49. M. Ahmad, T. King, D. Ko, B.H. Cha, J. Lee, Laser Technol. **34**, 445 (2002)
50. R. Fan, X. Li, Y. Xia, Y. Jiang, W. He, D. Chen, Chin. Phys. Lett. **25**, 1881 (2008)